SAND2000-2895C

USING MICROELECTRODES TO DETERMINE THE AVAILABILITY AND BEHAVIOR OF PIT INITIATION SITES IN ALUMINUM

F. D. Wall, M. A. Martinez
Sandia National Laboratories
P.O. Box 5800
Albuquerque, NM 87185-0888

ABSTRACT

A repetitive polarization experiment was developed which allows measurement of multiple pitting potentials from a single experiment. Automated data analysis is used to extract potentials relating to metastable and stable pit initiation. A multi-electrode sample was used to evaluate the dependence between subsequent pits in aluminum. It was found that the events have little or no dependence on prior sample history. The repetitive polarization experiment was used to evaluate the effect of sample size and purity on pit initiation in aluminum. Pitting potentials increased for decreasing sample size. No clear difference in pitting potential was observed for 99% and 99.99% purity Al. The presence of inclusions was not found to control pitting behavior.

INTRODUCTION

Pitting of aluminum is often studied using samples having relatively large surface areas (several mm^2 up to tens of cm^2) even though pit initiation occurs on a microscopic scale, and stable pits may only be several microns in diameter. Assuming that pit initiation is due to a heterogeneous distribution of flaws or defects in the Al oxide or in the underlying material, the larger a sample, the more likely that the entire distribution will be present. Thus, when a pitting potential is determined, the weakest site will dominate the sample response and give rise to the observed pit. Even if a large population of samples is tested, it is probable that only the lower tail of the true distribution of pitting potentials will be observed. This artifact may be beneficial in determining pitting behavior for engineering applications as it yields a conservative estimate of a "safe" potential range. However, to study the mechanism for pit initiation it is desirable to be able to explore the entire distribution of pitting potentials and how they relate to the local structure of the material and oxide. Also, for very small structures (i.e., microelectronics and micro-electromechanical machines), the distribution of pitting behavior determined using macroscopic samples may not be appropriate. It may be more useful to think in terms of failure probabilities taking into account sample size as well as material chemistry and environment.

Böhni and Suter used micro-capillaries to mask off very small areas (10^{-2} down to 10^{-6} cm^2) of samples and made standard 3-electrode measurements on stainless steels [1]. They reported currents in the 50 fA range corresponding to metastable pitting that would not have been detectable using larger electrode areas. Furthermore, they observed an increase in pitting potential as the surface area of the electrode was decreased. These

DISCLAIMER

DISCLAIMER

Portions of this document may be illegible in electronic image products. Images are produced from the best available original document.

results support the assumption of a population of defects controlling pit initiation. Other researchers agree with this hypothesis and have used statistical distributions to describe pitting behavior in terms of both induction time and pitting potential [2-8]. Unfortunately, gathering statistically significant quantities of data can be a daunting task. Induction times for metastable pits can be assessed using potentiostatic techniques but gathering large numbers of pitting potentials usually requires one sample per datum [9,10].

Previously, we reported a current-limited imposed-potential technique that enabled the collection of multiple pit initiation potentials from a single experiment [11]. The CLIP test functioned by limiting the available cathodic current to a pit site through a voltage divider scheme. The difficulty with the technique stems from the necessity to carefully choose a sample area and electronic circuitry that work correctly with the impedance of the native oxide. In the present work we show a new approach to gathering entire distributions of pitting potentials from single experiments. We also investigate the use of microelectrodes (down to 20 μm^2) to evaluate the area dependence of pitting potentials in pure Al. These techniques lend insight into the behavior of naturally occurring low defect density oxides, the behavior of repassivated pits, and the independence of pitting events.

EXPERIMENTAL

Materials

Al wire samples were used in the electrochemical testing. Wires were 500, 25 and 5 μm in diameter. Material purity ranged from 99% to 99.99% Al. Test solutions were prepared from reagent grade chemicals and 18 M-Ω water.

Electrode preparation

Wires were coated with an insulating electrophoretic paint (PPG, part # ED5050B). The paint was applied by immersing the wire and using a platinized niobium counter electrode to apply between –4 V and –10 V DC (vs. the counter electrode) for 120 s. The wires were then baked at 175°F for 1800 s to cure the paint. The resulting coating was adherent, continuous and electrically insulating and ranged in thickness from 4 to 10 μm. The coated wires were mounted in an epoxy resin mould for physical rigidity and ease of handling. Mechanical polishing down to 0.05 μm alumina was used to achieve a mirror finish. Some of the electrodes received a final two-part etch. For these electrodes, the surface was etched with 1 M NaOH for 300 s to remove any plastic deformation due to mechanical polishing. A final etch in 50% HNO_3 for 60 s was performed in order to promote a uniform oxide layer.

Repetitive polarization scans

Potentiodynamic experiments were performed in aerated 50 mMol NaCl solution at 25°C. Prior to running the scan, samples were polarized to a constant potential (generally –0.95 V_{SCE}) for a hold time ranging from 60 s to 600 s depending on the experiment. After the hold time elapsed, the potential was ramped in the anodic direction

at a sweep rate of 1 mV/s. The scan was terminated if a prescribed potential was reached or if the current flow from the sample exceeded a threshold. Most experiments used a current threshold of $2x10^{-7}$ A. Repetitive polarization experiments were run by repeatedly cycling through the above sequence. After each sweep, the potential was stepped back to the initial hold potential. Passive current density values and pitting potentials were determined for data sets using in-house, automated software. The solution in the vicinity of the sample surface was continuously stirred throughout the experiment by either bubbling ambient air in the solution or by recirculating solution using a peristaltic pump. This was done in an attempt to prevent any local alteration of the solution chemistry.

Multielectrode testing

A multielectrode was fabricated from 9 wires of 99% Al with diameters of 500 μm. These wires were arranged in a 3x3 array with several mm spacing between wires. A Scribner Associates Multi-Microelectrode Analyzer (MMA™) was used to short all 9 electrodes together through zero resistance ammeters (ZRA's) and simultaneously record the current flowing through each of the electrodes. The MMA™ was also used to control the applied potential and was programmed to perform the repetitive polarization experiment.

RESULTS AND DISCUSSION

An example of the raw data generated by a repetitive polarization scan (RPS) run for 999 iterations on 99.99% Al in 50 mMol NaCl is shown in Figure 1. Automated software is used to analyze the data for trends indicative of pitting. A minimum % change in the current value and a minimum absolute change in the current value between consecutive data points is used to identify pit initiation. The first time the data exceed the percent and absolute tolerances, the potential is recorded as the first instance of pit initiation. If the pit does not repassivate before the current limit is reached, then the potential where pitting initiated is recorded as the pitting potential. Finally, the potential being applied when the current limit is reached is recorded as the final potential and is indicative of the pit reaching an arbitrary stage of propagation. All three of these parameters are metrics for pitting susceptibility.

An example of analyzed data for 99.99% Al in 50 mMol NaCl is plotted as critical potential (first pit, pitting potential and final potential) vs. scan number in Figure 2.a. and as cumulative distribution functions in Figure 2.b. There is extensive overlap in the data, which is a result of the first pit initiated propagating quickly to the trigger current level. In this case the potentials for the first pit and last pit are identical and differ only slightly from the final potential. There is much more of a tail to the distribution for the first pit potential than for the other two values. This suggests that the minimum potential necessary for pit stabilization and propagation is bounded more tightly than the potential necessary for pit initiation. A micrograph of the sample surface following the 999 scans reveals some areas of high pit density and other areas of the sample devoid of pits all together (Figure 3). There are two plausible explanations for grouping of pit locations. One, a repassivated pit may serve as a preferential site for future pit initiation (either due to modification of the local solution chemistry or due to a less robust oxide than the original being formed upon repassivation). Two, clusters of pitting sites may

follow a defect structure inherent in the protective oxide or in the underlying material. If the former explanation is correct, then data from the RPS technique will not reflect the behavior of the original oxide.

One method to evaluate the propensity for a repassivated pit to serve as a preferential site for future pit initiation is to record the time and location of pitting events and determine if subsequent pits are occurring at the same approximate location. To accomplish this a nine-electrode sample was constructed from 500 μm diameter, 99% Al wires. The nine electrodes are electrically coupled so that they act as a single larger electrode. The current flow through each electrode is monitored using the MMA™ thus allowing the location of each pit to be known to within the area of a single wire (Figure 4). The pitting potential and location is recorded for each scan. These data are analysed to determine the number of times a given electrode pits in a row. Then the number of times that n pits occur in a row is tabulated (i.e., an experiment might have no consecutive pits occur 100 times, 2 consecutive pits occur 10 times, 3 pits 1 time, and no more than three pits in a row at any time in the experiment). Figure 5 shows the number of times n consecutive pits occurred during the experiment. For comparison, simulations were run where the probability of a site pitting consecutively was a controlled parameter of the simulation. The experimental data fall between the calculated lines for 0% and 5% of the repassivated pits being the preferential site for the next pit. These data indicate that the repassivated pits are not preferential sites for future pits. It is not clear from this experiment whether or not the repassivated pit could have an induction time then become a preferential site for future pitting. This issue will be addressed in more detail in a separate publication.

For the cases where consecutive pits do occur on a single electrode, it is of interest to know if the latter pits have lowered pitting potentials compared to the rest of the population. Figure 6 is a graph of the distribution of the difference between the pitting potential recorded in scan N and the pitting potential recorded in scan $N - X$. When X is set to 1 a comparison is made between subsequent pitting potentials. When X is set to an arbitrarily large number (i.e., 20), then the comparison represents the random distribution of the difference between pitting potentials. The graph shows almost identical distributions for $X = 1$ and $X = 20$ when pitting potentials from the entire population of data are used. The same distribution is also observed for $X = 1$ when only the data points from consecutive pits on the same electrode are used. This indicates that subsequent pits do not correlate to lowered pitting potentials and serves as further evidence that repassivated pits are not preferential sites for future pit initiation. It should be noted that analysis of time series of metastable pitting in both Al and stainless steel has shown non-Poisson behavior indicating interdependence of pitting events [12]. Though, in those experiments no measures were taken to flush the chemistry from the pitting site. We can thus reconcile our results which relate to the behavior of repassivated pits exposed to the bulk environment and the results of the cited work which relate to native oxide exposed to a locally altered chemistry.

The repetitive polarization experiment was used to evaluate the effects of electrode size and electrode purity on pitting potential distribution. Distributions for the pitting potential are given for Al wires having 500, 25 and 5 μm diameters in Figure 7. The 500 and 25 μm wires are 99.99% pure while the 5 μm wire is 99.95% pure. Although only 3 data points have been collected for the 5 μm wire, these data are still

shown as a CDF for comparison purposes. There is a clear difference between the distributions for the 500 μm wire and the two smaller wires. While there are not enough data to accurately describe the 5 μm wire, it is apparent that much higher pitting potentials may be observed for this sample size than for the larger diameter samples. Thus these data agree with the trend of increasing pitting potential with decreasing diameter observed by Böhni and Suter using capillary cells to test stainless steel [1].

The effect of electrode purity on pitting potential distribution is shown in Figure 8.a. for 500 μm wires and in Figure 8.b. for 25 μm wires. There is no clear difference in the span of pitting potentials for 99% and 99.99% Al. The distribution for 99% Al is weighted towards slightly higher pitting potentials for the 500 μm wires, however, for the 25 μm wires the distribution for 99% Al is shifted toward slightly *lower* potentials. That the lower purity may display as good as or better pitting resistance that the higher purity Al is in conflict with conventional views. However, recent work by Fecke on various purity Al alloys has also shown pitting potential to scale inversely with purity [13]. This raises the question of whether or not inclusions in the high purity Al are preferential sites for pit initiation during controlled potential experiments. Figures 9.a. and 9.b. show micrographs of 99% and 99.99% Al samples that were pitted 5 times each. Although the 99% sample (Fig. 9.a.) contains numerous Fe-rich inclusions and is clearly not as clean as the 99.99% Al (Fig 9.b.), the pitting potentials recorded were generally higher for the 99% Al. Thus, the mere presence of these inclusions does not control the pitting behavior of Al.

SUMMARY

The repetitive polarization scan technique provides a means of acquiring entire distributions of pitting potentials from a single electrode in a single experiment. Although the sample is pitted numerous times, analysis of a multi-electrode sample has shown that the repassivated pits do not skew the subsequent behavior of the sample. Thus repassivated pits are not preferential sites for future pit initiation, indicating that the oxide formed upon repassivation is at least as robust as the native oxide. Testing of 500, 25 and 5 μm samples has shown that pitting potential increases with decreasing surface area for high purity aluminum samples. Similar distributions in pitting potential were found for 99% and 99.99% Al samples even though the 99% sample has a much higher Fe-rich inclusion content. These preliminary results suggest that the presence of these inclusions does not control the pitting potential of the sample.

REFERENCES

1. H. Böhni, T. Suter, A. Schreyer, Electrochimica Acta., **40**, 1361 (1995).
2. N. Sato, *J. Electrochem Soc.*, **123**, 1197 (1976).
3. H. S. Isaacs and Y. Ishikawa, *J. Electrochem. Soc.*, **132**, 1288 (1985).
4. G. S. Frankel, L. Stockert, F. Hunkeler and H. Boehni, *Corrosion*, **43**, 7, 429 (1987).
5. A. M. Riley, D.B. Wells and D. E. Williams, *Corrosion Science*, **32**, 12, 1307 (1991).
6. U. Bertocci, M. Koike, S. Leigh, F. Qiu and G. Young, *J. Electrochem. Soc.*, **133**, 1782 (1986).
7. S. T. Pride, J. R. Scully and J. L. Hudson, *J. Electrochem. Soc.*, **141**, 3028 (1994).

8. D. E. Williams and C. Westcott, *Metallic Corrosion*, **4**, Proceedings of the 9th ICMC, National Research Council of Canada, Toronto, 390 (1984).
9. T. Shibata and T. Takeyama, *Corrosion*, **33**, 7, 243 (1977).
10. C. Blanc, B. Lavelle and G. Mankowski, *Corrosion Science*, **39**, 3, 495 (1997).
11. F. D. Wall, *Current-Limited Imposed-Potential Technique for Inducing and Monitoring Metastable Pitting Events*, Proc. Vol. 1999 of the 196th Meeting of The Electrochemical Society and 1999 Fall Meeting of the Electrochemical Society of Japan, Honolulu, HI, Oct. 1999.
12. T. T. Lunt, S. T. Pride, J. R. Scully, J. L. Hudson, *J. Electrochem. Soc.*, **144**, 5, 1620 (1997).
13. Rob Fecke, Masters Thesis, Ohio State University, to be published.

This work was supported by the DOE Office of Basic Energy Sciences (BES). Sandia is a multiprogram laboratory operated by Sandia Corp., a Lockheed Martin Co., under U.S. DOE contract DE-AC04-94AL85000.

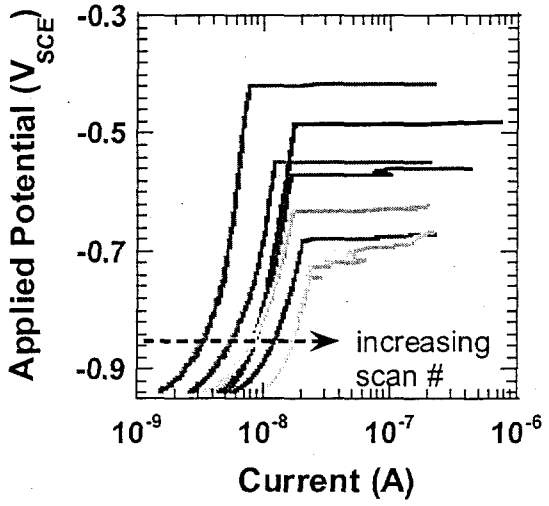

Figure 1. An example of the raw data collected during a RPS experiment. 99.99% Al in 50mMol NaCl @ 25°C. Passive current increases with scan number. The pitting potential is not a strong function of scan number (see Figure 2).

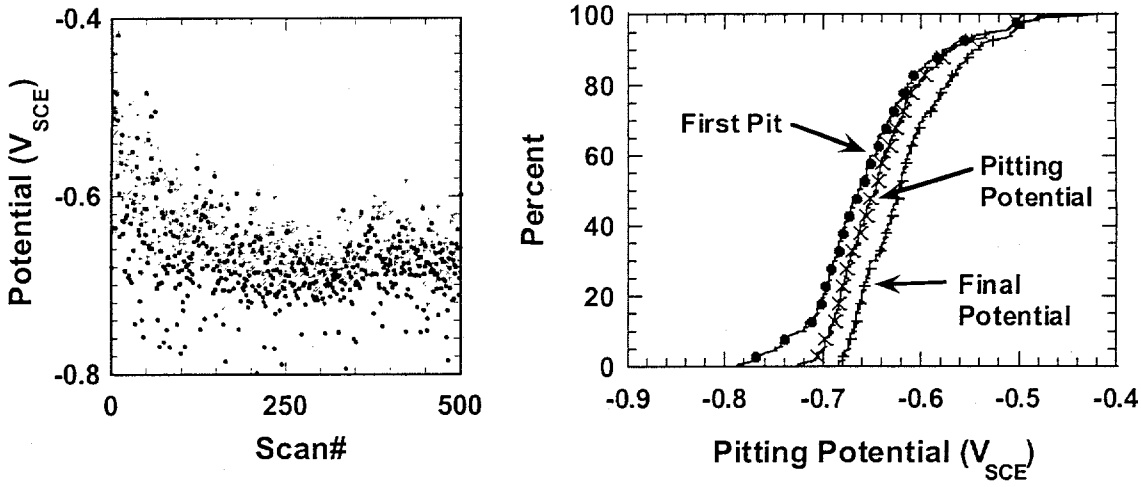

(a) (b)

Figure 2. 99.99% Al in 0.05M NaCl @ 25°C. RPS experiment run with 600 s holds at -0.950 V_{SCE} followed by anodic scans @ 1 mV/s terminated for $I > 2x10^{-7}$ A. First pit initiation detected (•), pitting potential (×) and final potential (+). (a) Critical potentials vs. scan number and (b) cumulative distribution functions.

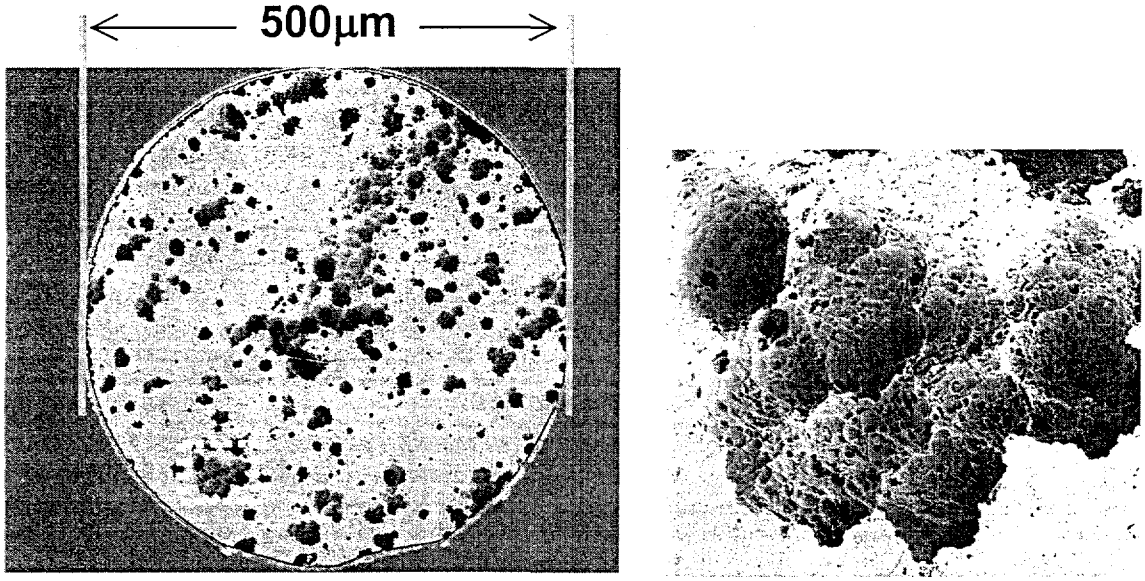

(a) (b)

Figure 3. SEM micrograph of 99.99 sample after RPS testing with 999 scans. (a) Overview of sample surface showing clustering of pits. (b) Close-up of pit cluster outlined with dashed line in 'a'.

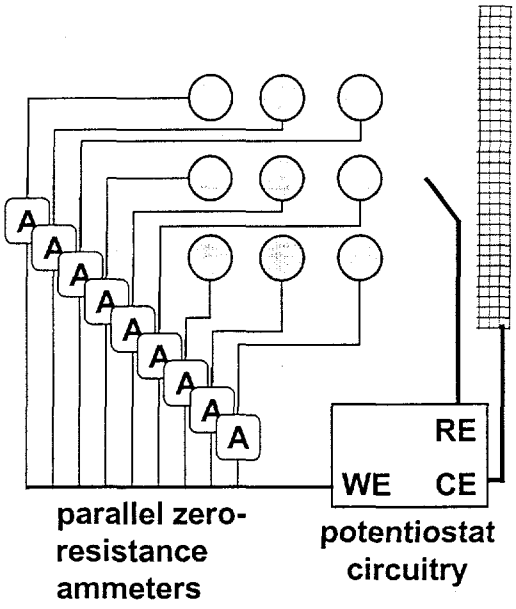

Figure 4. Nine Al wires arranged in 3x3 pattern to form a multi-electrode. The current through each wire is independently monitored with individual ZRA's. All wires are electrically shorted to act as a single working electrode.

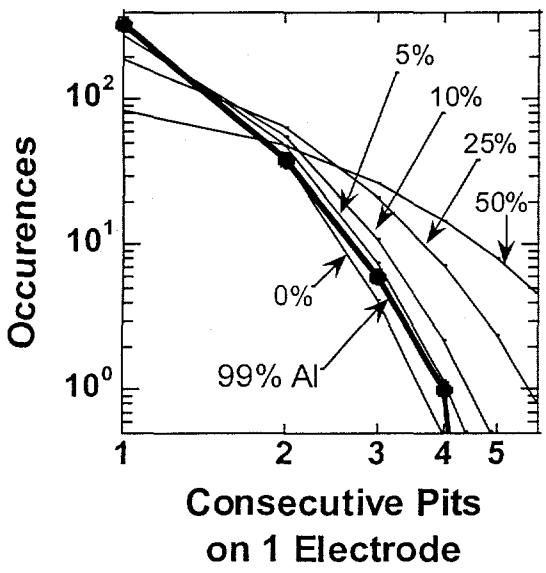

Figure 5. Frequency of consecutive pits on a single electrode for 3x3 array of 99% Al wires. Simulated data are used to show the predicted frequencies of consecutive pits. The probability indicates the chance that a pit will predispose the electrode to pit during the next scan.

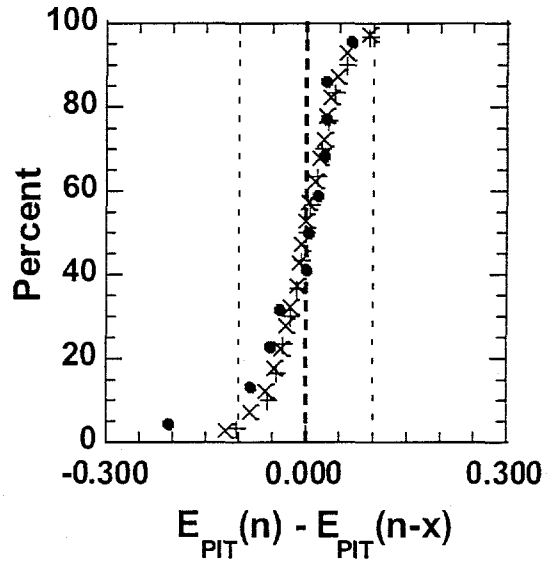

Figure 6. Distributions of the difference between pitting potentials separated by X scans. (+) All scans analysed with X=1, (×) all scans analysed with X=20, and (•) consecutive pits analysed with X=1.

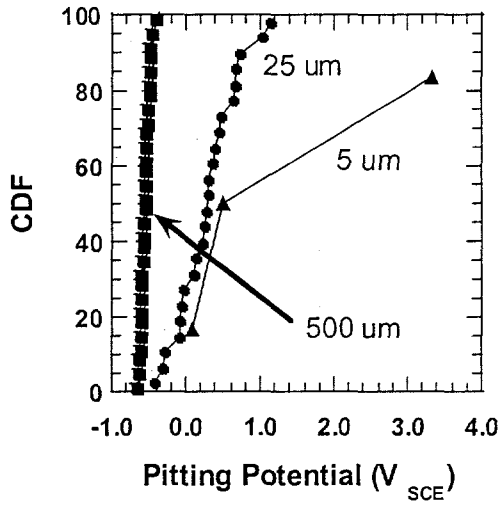

Figure 7. Distributions of pitting potentials for Al wires having diameters of (■) 500 μm, (●) 25 μm and (▲) 5 μm. The 500 and 25 μm wires are 99.99% pure and the 5 μm wire is 99.95% pure. Wires tested in 50 mMol NaCl @ 25°C with a scan rate of 1 mV/s. These data indicate that many regions of the Al samples have very robust oxides and elevated pitting potentials compared to those observed on larger samples.

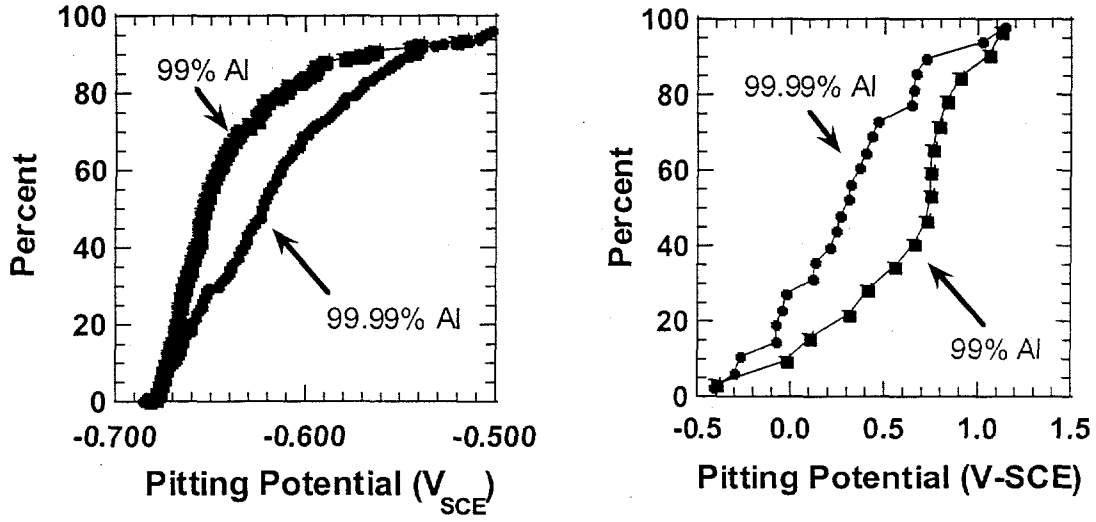

Figure 8. Effect of electrode purity on pitting potential distribution. For 500 μm diameter wires (a) the distribution is shifted to slightly higher potentials for the 99.99% Al, whereas for 25 μm wires (b) the distribution is slightly higher for the 99% Al.

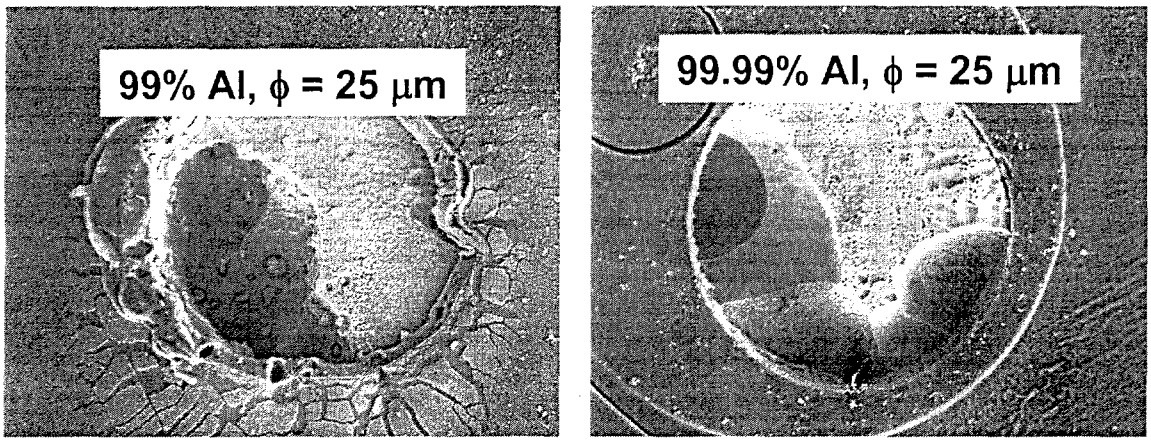

(a) (b)

Figure 9. SEM micrographs of (a) 99% Al and (b) 99.99% Al after RPS testing for 5 scans each in 50 mMol NaCl solution @ 25°C. The pitting potentials for the 99% Al were, in general, higher than those for the 99.99% Al even though the lower purity material appears to contain a higher volume fraction of inclusions.